Astro. Lett. and Communications, 1995, Vol. 32, pp. 223–228
Reprints available directly from the publisher
Photocopying permitted by license only

The Millimeter Wave Anisotropy Experiment (MAX)

S. TANAKA[1,2], D. ALSOP[1,2], E. CHENG[3], A. CLAPP[1,2], D. COTTINGHAM[1,2], M. DEVLIN[1,2], M. FISCHER[1,2], J. GUNDERSEN[1,4], C. HAGMANN[1,2], W. HOLMES[1,2], V. HRISTOV[1,2], T. KOCH[4], E. KREYSA[5], A. LANGE[1,2], M. LIM[1,4], P. LUBIN[1,4], P. MAUSKOPF[1,2], P. MEINHOLD[1,4], P. RICHARDS[1,2], G. SMOOT[1,6] and P. TIMBIE[1,2]

[1] *The Center for Particle Astrophysics, University of California, Berkeley, CA 94720;* [2] *Department of Physics, University of California, Berkeley, CA 94720;* [3] *NASA Goddard Space Flight Center, Greenbelt, MD 20771;* [4] *Department of Physics, University of California, Santa Barbara, CA 93106;* [5] *Max-Planck-Institut für Radioastronomie, Auf dem Hügel 69, D-5300 Bonn 1, Germany;* [6] *Lawrence Berkeley Laboratory, Berkeley, CA 94720.*

(Received 4 January 1994; in final form 7 September 1994)

The balloon-borne Millimeter Wave Anisotropy Experiment (MAX) observes fluctuations in the cosmic microwave background (CMB) on one degree angular scales. Measurements at these angular scales constrain scenarios of large scale structure formation. This paper presents an overview of the MAX experiment and the data obtained thus far from the four flights of the MAX experiment.

KEYWORDS: Cosmic microwave background–cosmology: observations

HISTORY OF THE MAX EXPERIMENT

There have been four successful flights of the MAX instrument. The first flight in 1989 (MAX1) yielded systematic tests of instrument performance and placed an upper limit to CMB fluctuations (Fischer *et al.*, 1992). The second flight in 1990 (MAX2) included a scan of a low dust contrast region near the star Gamma Ursa Minoris (GUM) ($\alpha = 15\,\mathrm{h}$, $20.7\,\mathrm{m}$, $\delta = 71°52'$, epoch, 1991) where we observed significant structure (Alsop *et al.*, 1992). The third flight in 1991 (MAX3) included another scan of the GUM region which yielded structure of comparable amplitude (Gundersen *et al.*, 1993). This flight also included a scan of a higher dust contrast region near the star Mu Pegasi ($\alpha = 22\,\mathrm{h}\,50\,\mathrm{m}$, $\delta = 24°33'$, epoch, 1991) (Meinhold *et al.*, 1993a) which yielded an upper limit to CMB fluctuations smaller than the amplitude measured in the GUM region. During the most recent flight in 1993 (MAX4), we scanned the GUM region a third time (Devlin *et al.*, 1994). This paper presents preliminary results from that scan. MAX4 also included scans of two additional low dust contrast regions near the stars Sigma Herculis ($\alpha = 16\,\mathrm{h}$, $34.1\,\mathrm{m}$, $\delta = 42°26'$, epoch, 1993) and Iota Draconis ($\alpha = 15\,\mathrm{h}\,24.9\,\mathrm{m}$, $\delta = 58°58'$, epoch, 1993) (Clapp *et al.*, 1994).

INSTRUMENT

We have described the MAX instrument in detail elsewhere (Fischer *et al.*, 1992; Alsop *et al.*, 1992; Meinhold *et al.*, 1993b). The instrument is a multiband bolometric receiver mounted on an attitude-controlled, balloon-borne telescope. A one meter parabolic primary with a nutating elliptical secondary are used in an underfilled off-axis Gregorian configuration.

In MAX1–3 the underfilled optics provide a 0.5° FWHM beam in all optical bands. The chopping secondary sinusoidally modulates the beam in azimuth at 6 Hz with a 1.3° peak to peak throw on the sky. The 300 mK ^{3}He-cooled bolometric photometer has three optical bands centered at 6, 9 and 12 cm^{-1}. Bolometers allow a large spectral range to be divided into several bands. We designed the optical bands to maximize spectral discrimination and sensitivity to CMB.

In the present MAX4 configuration we extended our spectral coverage with a 0.6° FWHM beam in a single mode band at 3 cm^{-1} in addition to 0.8° FWHM beams in the multimode 6, 9 and 14 cm^{-1} bands. The 3 cm^{-1} band is sensitive to CMB and also provides low frequency spectral discrimination. Additionally, the high frequency band center was shifted from 12 cm^{-1} to 14 cm^{-1} to provide better dust discrimination. An adiabatic demagnetization refrigerator cools the photometer to 85 mK in an effort to increase bolometer sensitivity.

During observations of the CMB, the attitude control system smoothly scans the center of the chopped beam 6° peak to peak in azimuth while tracking a fiducial point in elevation. The sky rotates through our beam during CMB scans that last over an hour, producing a bow-tie pattern on the sky.

WINDOW FUNCTION AND CALIBRATION

The window function of the MAX experiment is needed in order to compare MAX results to cosmological models and to other experiments at different angular scales. This section describes some of the experimental determinants of the MAX window function. The beam size and chop amplitude determine the chopped beam pattern. We verify our chopped beam pattern in flight with a scan of a planet, such as Jupiter. The chopping secondary mirror sinusoidally modulates the beam at 6 Hz. Using the secondary mirror position as its reference, a sine wave lock-in outputs both the in phase and out of phase components at the fundamental chopper frequency:

$$V_{\text{out}}(\theta = 0) = \int V_{\text{bolo}}(t) \times \sin(\omega t)\, dt \qquad \text{(in phase)}$$

$$V_{\text{out}}\left(\theta = \frac{\pi}{2}\right) = \int V_{\text{bolo}}(t) \times \sin\left(\omega t + \frac{\pi}{2}\right) dt \qquad \text{(out of phase)}$$

An in-flight membrane calibration converts voltage signal to temperature difference on the sky as shown in Figure 1. In lab we measure the reflectance R of 12.5 μm thick polypropylene membrane in our frequency bands. During flight a motor steps this partially reflecting membrane into the beam at the prime focus. The membrane reflects

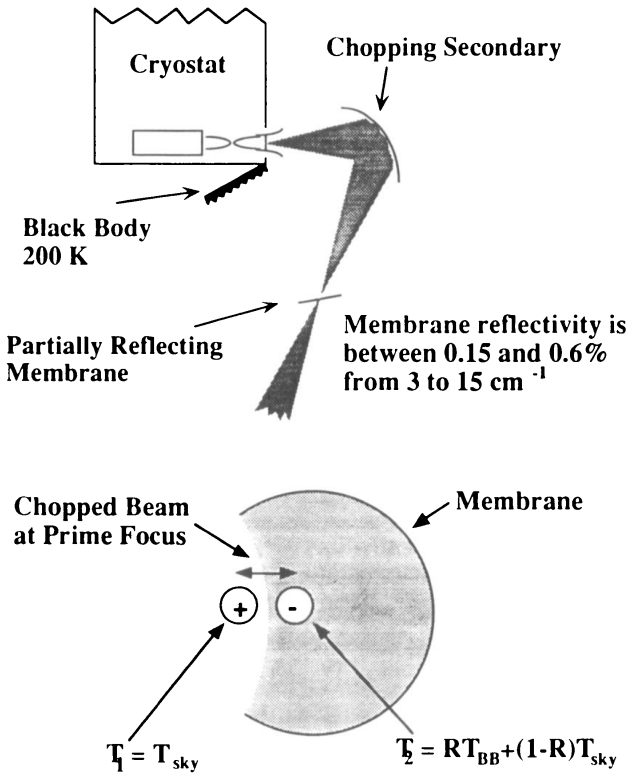

FIGURE 1 In flight membrane calibration.

light from a blackbody whose temperature is monitored into the receiver. The secondary mirror chops on and off the membrane, corresponding to a peak to peak temperature difference $\Delta T_{\text{calibration}} = T_{\text{sky}} - T_{\text{membrane}}$ where

$$T_{\text{membrane}} = RT_{\text{blackbody}} + (1 - R)T_{\text{sky}}.$$

During the membrane calibration we measure a voltage signal $V_{\text{calibration}}$. These measured values calibrate the rest of the data rom voltage to temperature difference:

$$\Delta T_{\text{out}} = \frac{V_{\text{out}}}{V_{\text{calibration}}/\Delta T_{\text{calibration}}}$$

Signals from planets with known brightness temperatures and angular diameters are used to check this calibration.

RESULTS

Mu Pegasi (MAX3)

The data collected in the high frequency band of the Mu Pegasi scan strongly correlate with the morphology of IRAS 100 μm dust. In a two component fit of dust and CMB, both components have comparable magnitudes. This fit places an 95% confidence level

upper limit on CMB anisotropy of $\Delta T_{rms}/T_{CMB} = 2.5 \times 10^{-5}$ for a Gaussian autocorrelation function with coherence angle $\theta_c = 25'$.

In addition to providing an upper limit to CMB fluctuations in one region of sky, the Mu Pegasi measurement demonstrates that the experiment can correctly measure low level signals, and it places limits on the dust emission expected in other scans. The measurement of the dust scales the IRAS 100 μm maps to the MAX frequency bands. In the Mu Pegasi region we measured $\Delta T_{dust}/T_{CMB} = 1.8 \times 10^{-5}$. This scaling corresponds to a dust contribution in the GUM region of $\Delta T_{dust}/T_{CMB} = 6 \times 10^{-6}$ and in the lowest dust contrast regions in the sky of $\Delta T_{dust}/T_{CMB} = 2 \times 10^{-6}$.

The Mu Pegasi measurement also places limits on possible sidelobe contamination. This scan covers a wider range of elevations than the GUM scan, and there is no detected signal change as a function of elevation. The total amplitude of the Mu Pegasi fluctuations is also less than that measured near GUM.

GUM

We have scanned regions of the sky centered on GUM in MAX2, MAX3 and MAX4. Because of the effects of sky rotation these regions do not overlap. In all three flights we have measured significant correlated structure in the 6 and 9 cm^{-1} bands for MAX2 and MAX3 and in the 3, 6 and 9 cm^{-1} bands for MAX4. The measured antenna temperature of the structure decreases as a function of frequency as is expected for CMB anisotropy.

The MAX2 GUM scan differs from the other scans discussed because of scan strategy and data filtering. The scan strategy used for MAX2 was a step scan in azimuth rather than a smooth scan. Also, we applied a high pass filter on the data to remove 1/f noise due to chopper instability. In this region we measured $\Delta T_{rms}/T_{CMB} = 3 \times 10^{-5}$. If we assume that all the structure is CMB anisotropy, this measurement corresponds to $\Delta T/T_{CMB} = 4.5 \pm {}^{6.5}_{2.5} \times 10^{-5}$ for a Gaussian autocorrelation function with coherence angle $\theta_c = 25'$ where the $\pm$ refer to the 95% confidence level upper and lower limits.

Because we observed significant structure in the MAX2 GUM scan, we returned to this region during MAX3. We measured $\Delta T_{rms}/T_{CMB} = 4.7 \pm 0.8 \times 10^{-5}$. If we assume all the structure is CMB anisotropy, this measurement corresponds to $\Delta T/T_{CMB} = 4.2 \pm {}^{1.7}_{1.1} \times 10^{-5}$ for a Gaussian autocorrelation function with coherence angle $\theta_c = 25'$ where the $\pm$ refer to the 95% confidence level upper and lower limits. The differences in experimental strategy give differences in ΔT_{rms} for data with very similar values of the Gaussian autocorrelation function.

If we assume that all the structure is CMB anisotropy, the CMB temperature rms values measured near GUM in MAX4 are 3.6×10^{-5}, 1.8×10^{-5}, and 2.3×10^{-5} in the 3, 6 and 9 cm^{-1} bands which have full width half maximum beam widths of 0.6°, 0.8° and 0.8°, respectively. These rms values do not include correction for the different beam widths. The analysis on this data set is still in progress.

The falling spectrum of the observed structure eliminates atmospheric contamination, 20 K interstellar dust emission, and Rayleigh-Jeans sources. Amplitude arguments eliminate the possibility of significant signal from point sources in the region. The edge of the MAX3 GUM scan intersects the quasar 3C309.1. Measurements of the

quasar at 80 and 230 GHz (Steppe *et al.*, 1988) predict an amplitude in our 6 cm^{-1} band that is 30 times smaller than the observed structure. Furthermore, deletion of the quasar pixels does not affect the $\Delta T_{rms}/T_{CMB}$ at 6 cm^{-1}.

Amplitude arguments also eliminate the possibility of significant signals from synchrotron radiation and free-free emission. Assuming that the antenna temperature due to synchrotron radiation scales as $\nu^{-2.7}$, extrapolation from a Haslam map convolution predicts an amplitude 100 times smaller than we measure. Similarly, assuming free-free antenna temperature scales as $\nu^{-2.1}$, extrapolation from a Haslam map convolution predicts an amplitude 30 times smaller than we measure. Measurements of $H\alpha$ emission by Reynolds (1992) suggest that in the most extreme case at our galactic latitude and angular scale, the estimated amplitude is 10 times smaller than the observed structure. These arguments regarding galactic confusion are given in more detail in Gundersen *et al.* (1993). As reported at this conference, observations by the Cambridge Anisotropy Telescope (CAT) (Lasenby *et al.*, 1993) provide the most conclusive evidence that the observed structure is due to neither synchrotron emission nor free-free emission. CAT observed a $2.5° \times 2.5°$ region of sky centered on GUM with a 0.5° beam and measured a temperature less than 300 μK_{rms} at 15 GHz. If the synchrotron or free-free emission caused the structure in our bands, the CAT would measure much higher temperature fluctuations at this lower frequency.

FUTURE OF MAX

The capabilities of the MAX experiment expand with each successive flight. In the spring of 1994 we will fly the ADR receiver again with plans to improve the detector sensitivity and to increase the sky coverage of our anisotropy measurements to reduce the effect of sampling variance. In parallel, we are developing a new telescope and a new array receiver.

The new telescope consists of a 1.3 m diameter, off-axis, paraboloidal primary mirror. The chopper drive can modulate the lightweight mirror at 3 Hz with variable amplitudes as large as 5°. Unlike the chopping secondary mirror, the chopping primary mirror will chop neither the emissivity gradient across the primary mirror nor the diffraction spillover. The absence of chopping aberrations meets the requirements of the array receiver.

The bolometric array receiver will have 8 four-color pixels. Each pixel will have the same sensitivity as the present 85 mK receiver. The array receiver will have the capability to make sensitive maps of detected anisotropies, thus allowing the study of the morphology of any anisotropic structure.

ACKNOWLEDGMENTS

This work was supported by the National Science Foundation through the Center for Particle Astrophysics (cooperative agreement AST-9120005), the National Aeronautics and Space Administration under grants NAGW-1062 and FD-NAGW-2121, the University of California, and previously by the California Space Institute.

REFERENCES

Alsop, D. *et al.*, 1992, *Astrophys. J.*, **317**, 146.
Clapp, A. *et al.*, 1994, *Astrophys. J.*, **433**, L57.
Devlin, M. *et al.*, 1994, *Astrophys. J.*, **430**, L1.
Fischer, M. *et al.*, 1992, *Astrophys. J.*, **388,** 242.
Gundersen, J. *et al.*, 1993, *Astrophys. J.*, **413**, L1.
Lasenby, A. *et al.*, 1993, Private communication.
Meinhold, P. *et al.*, 1993a, *Astrophys. J.*, **409,** L1.
Meinhold, P. *et al.*, 1993b, *Astrophys. J.*, **406,** 12.
Reynolds, R. J., 1992, *Astrophys. J.*, **392,** L35.
Steppe, H. *et al.*, 1988, *Astron. Astrophys. Space*, **75,** 317.